

Split of spatial attention as predicted by a systems-level model of visual attention

Marc Zirnsak,¹ Frederik Beuth² and Fred H. Hamker²

¹Department of Neurobiology, Stanford University School of Medicine, Stanford, CA, USA

²Department of Computer Science, Artificial Intelligence, Chemnitz University of Technology, Straße der Nationen 62, 09107 Chemnitz, Germany

Keywords: frontal eye field, split of attention, visual search

Abstract

Can we attend to multiple distinct spatial locations at the same time? According to a recent psychophysical study [J. Dubois *et al.* (2009) *Journal of Vision*, 9, 3.1–11] such a split of spatial attention might be limited to short periods of time. Following N. P. Bichot *et al.* [(1999) *Perception & Psychophysics*, 61, 403–423] subjects had to report the identity of multiple letters that were briefly presented at different locations, while two of these locations (targets) were relevant for a concurrent shape comparison task. In addition to the design used by Bichot *et al.* stimulus onset asynchrony between shape onset and letters was systematically varied. In general, the performance of subjects was superior at target locations. Furthermore, for short stimulus onset asynchronies, performance was simultaneously increasing at both target locations. For longer stimulus onset asynchronies, however, performance deteriorated at one of the target locations while increasing at the other target location. It was hypothesized that this dynamic deployment of attention might be caused by competitive processes in saccade-related structures such as the frontal eye field. Here we simulated the task of Dubois *et al.* using a systems-level model of attention. Our results are consistent with recent findings in the frontal eye field obtained during covert visual search, and they support the view of a transient deployment of spatial attention to multiple stimuli in the early epoch of target selection.

Introduction

Despite an increasing number of studies arguing in favour of a split of spatial attention (e.g. Kramer & Hahn, 1995; Bichot *et al.*, 1999; Awh & Pashler, 2000; Gobell *et al.*, 2004; Dubois *et al.*, 2009) the debate whether their results truly provide evidence for a simultaneous employment of spatial attention at non-contiguous locations is still ongoing. For example, Jans *et al.* (2010) hypothesized that the observations by Bichot *et al.* (1999) and Dubois *et al.* (2009) could in principle be explained by a unitary, elliptical focus of attention encompassing the two target but none of the distractor stimuli.

The question of if and to what extent a split of attention is a useful interpretation of the reported observations has to address the neural structures involved in orientating covert spatial attention rather than just arguing on basis of hypothetical attentional foci. Converging evidence points to a critical role of brain areas that are involved in the control of eye movements. Moore & Fallah (2001) were the first to demonstrate that microstimulation of the macaque frontal eye field (FEF) increased performance in an attention-demanding task. Importantly, this increase was observed during subthreshold stimulation without evoking eye movements and was limited to locations corresponding to the response field of the respective FEF site. Similar results of space-specific benefits have been reported during microsti-

mulation of the superior colliculus (SC) (Muller *et al.*, 2005; Cavanaugh *et al.*, 2006). In addition to an increased performance and similar to effects observed during covert orienting of spatial attention (McAdams & Maunsell, 1999; Reynolds *et al.*, 2000; Buffalo *et al.*, 2010), microstimulation of corresponding FEF sites has been shown to enhance the responses to receptive field stimuli of V4 neurons (Moore & Armstrong, 2003). Related effects have also been reported in humans, as revealed by transcranial magnetic stimulation (Grosbras & Paus, 2002; Muggleton *et al.*, 2003; Smith *et al.*, 2005; Silvanto *et al.*, 2006; Taylor *et al.*, 2007).

Consistent with the observation that activity in oculomotor-related areas such as the FEF influences the representation of stimuli in visual areas, Hamker (2003, 2004a, 2005a,b) developed a computational framework in which attention-related phenomena are described by the interactions of different areas. In this framework, a ‘final’ selection in space is the result of a dynamic process resolving competition between different cell populations by means of continuous feedback in both the space and the feature domain, in concert modulating the bottom-up activity (Bichot *et al.*, 2005).

Although previous versions of the model were more in line with a strict version of the premotor theory of attention (Rizzolatti *et al.*, 1987) in the sense that the deployment of a spatial bias is essentially a planned but not executed eye movement, in particular mediated by movement or burst cell activity, dissociations between spatial selection and movement preparations suggesting an earlier visual component of spatial attention have recently been reported (Sato & Schall, 2003;

Correspondence: Dr F. H. Hamker, as above.
E-mail: fred.hamker@informatik.tu-chemnitz.de

Received 8 January 2011, revised 17 March 2011, accepted 31 March 2011

Juan *et al.*, 2004; Ray *et al.*, 2009). Accordingly, in the present version of the model we have reformulated the FEF. In particular, we included a new map of visuomovement cells with characteristics ranging from strong visual to more motor-related responses providing the spatial feedback signal. We show that the new model both is consistent with recent FEF findings during covert search (Monosov & Thompson, 2009) and accounts for the reported transient split of attention reported by Dubois *et al.* (2009).

Materials and methods

Model overview

The model consists of visual area 4 (V4), inferior temporal cortex (IT), prefrontal areas that contain the FEF for saccade planning and more ventrolateral parts involved in executive control (Fig. 1). If we present a visual scene to the model, features such as colour, intensity and orientation are computed from the image. The fact that features that are unique in their environment ‘pop-out’ is accounted for by computing an initial stimulus-driven saliency which determines the input into V4 (Burrows & Moore, 2009). We consider this stage a simplification with respect to its location in the brain. Pop-out effects are not necessarily generated early in the visual pathway. They are probably also computed in later areas, such as IT.

Feature and salience information are both encoded within a population of cells at each position in space, where the presence and salience of a feature is represented by the rate of each feature-tuned cell. The growing receptive field size along the processing hierarchy requires that a number of V4 cells project to a single IT cell. In addition to bottom-up projections, feedback from the FEF and IT increases the gain of the cells in V4. Search in this model can be goal directed as IT receives feature-specific feedback from the prefrontal (PF) cells, similar to that suggested by Chelazzi *et al.* (1998). As a result, those V4 cells that contain a target stimulus in their receptive field will show an enhanced response, similar as by Motter (1994) for

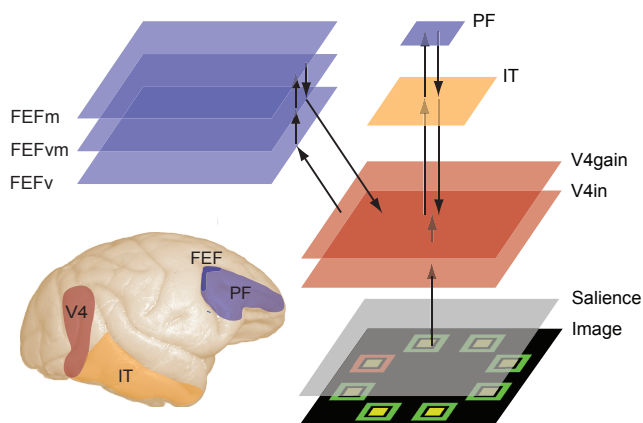


FIG. 1. Model layout. The input image is processed by a set of filters resulting in feature conspicuity values across different spatial scales for a given channel, which provides the V4in activity. The activity in V4gain is a function of the bottom-up input provided by V4in and top-down modulations provided by IT (which in turn can be biased by the PF) and the top-down modulations of the FEF. Thereby, the feedback signal from IT is feature specific whereas the feedback signal from the FEF is space specific. The FEF consists of three layers whose cells differ in their response characteristics. Cells in the FEFv layer are responsive to a visual stimulus but show no motor-related activity. Cells in the FEFm layer show no early transient response to visual stimulation but built up their activity during later stages of the selection process if not suppressed by fixation cells. Finally, cells in the FEFvm layer vary along a continuum of stimulus- and motor-related responses.

colour search. This feature bias in V4 is transferred into a location bias by the feedforward projection from V4 to the FEF. Object recognition in the ventral pathway of this model is strongly simplified, as the complexity of features does not increase from V4 to IT.

The planning of an eye movement is implemented as follows. The FEF visual (FEFv) neurons receive convergent afferents from V4. Input activity at each location is summed across all dimensions (e.g. colour and orientation). The firing rate of these cells represents the saliency and task-relevance of a location. In extension to the original model (Hamker, 2005a,b) FEF visuomovement (FEFvm) cells are now modelled in a continuum from low to high visual selectivity by a feedforward excitation and surround inhibition from the FEFv cells. FEFvm projects to FEF movement (FEFm) cells, which compete for the selection of the ‘strongest’ location and a saccade is initiated after exceeding a certain threshold. However, in the following studies they are strongly inhibited by fixation cells and thus are inactive. Modulatory spatial feedback into V4 (Hamker, 2004b) now originates in FEFvm cells and not FEFm cells as in previous versions.

Although some recent models of the FEF aimed at modelling the layered architecture (Brown *et al.*, 2004; Heinzle *et al.*, 2007) our focus is particularly at the functional level by realistically modelling the response profiles of some of the known cell properties, here in particular the visuomovement cells. However, a rough assignment to layers can also be given in our model: FEFv relate to cells in layer 4 and layer 2/3, FEFvm model cells in layer 2/3 and FEFm are typically responses of cells in layer 5 (Segraves & Goldberg, 1987). A more detailed consideration of the FEF microcircuit must be taken with caution, as sufficient details are not known. For example, Heinzle *et al.* (2007) took the circuit of cat visual cortex and adjusted it to enable FEF functionality. Their responses of cells in layer 2/3 show little similarity to reported responses of visuomovement cells in the macaque monkey. Moreover, implemented versions of the layered models (Brown *et al.*, 2004; Heinzle *et al.*, 2007) have been simulated only with relatively simple input scenes.

Model equations

In the following, we provide a concise mathematical summary of the model and introduce the further developed FEF. For a detailed description of the remaining parts see Hamker (2005b). The firing rates of all neurons are written as $r_{d,i,x}^{\text{map}}$. The superscript denotes a particular map or area and the subscript denotes the neurons’ indices. The spatial position (x_1, x_2) of a given cell within a map is written as x , the index d defines a specific feature space called channel (blue–yellow, red–green, orientation, intensity) and the index i defines the preference for a particular feature in a certain channel. A single weight, connecting neurons from two different maps, is termed as $w^{\text{map1} \rightarrow \text{map2}}$, where map1 contains the ‘presynaptic’ neuron and map2 the ‘postsynaptic’ one. Spatial-lateral weight matrices are termed as $w_{x,x'}^{\text{map}/x}$ and weights in feature space, i.e. weights connecting cells at a given spatial position in a given channel are termed as $w_{i,i'}^{\text{map}/i}$. The function $(.)^+$ sets negative values to zero and the function $x^{\text{map}} \in RF(x)$ returns all neuron indices x' of the given map which are enclosed by the receptive field of x .

Visual area 4 gain (V4gain)

The change in a firing rate $\partial r_{d,i,x}^{\text{V4gain}} / \partial t$ consists of an excitatory term G and an inhibitory term H . The term G describes the feedforward influence from V4in (Eqn 1, line 1), the self-excitation among the features and within space (Eqn 1, line 2), the spatial feedback from FEFvm (Eqn 1, line 3) and the feature-based feedback from IT (Eqn 1, line 4).

$$\tau^{V4gain} \frac{\partial r_{d,i,x}^{V4gain}}{\partial t} = G - H; \quad r = (r)^+;$$

$\forall d, i, x:$

$$\begin{aligned} G_{d,i,x} &= w^{V4in-V4gain} r_{d,i,x}^{V4in} \\ &+ w^{V4in-V4gain} r_{d,i,x}^{V4in} \left(\sum_{i'} w_{i,i'}^{V4gain/i} r_{d,i',x}^{V4gain} + \sum_{x'} w_{x,x'}^{V4gain/x} r_{d,i,x'}^{V4gain} \right) \\ &+ \left(A - \max_{i'} \left(r_{d,i',x}^{V4gain} \right) \right) + r_{d,i,x}^{V4in} w^{FEFvm-V4gain} \sum_{x' \in RF(x)} \bar{r}_{x'}^{FEFvm} \\ &+ \left(A - \max_{i'} \left(r_{d,i',x}^{V4gain} \right) \right) + r_{d,i,x}^{V4in} w^{IT-V4gain} \max_{x' \in RF(x)} \left(r_{d,i,x'}^{IT} \right) \quad (1) \end{aligned}$$

The lateral excitatory weights in feature space are constructed by

$$w_{i,i'}^{V4gain/i} = 0.2 \exp\left(-\frac{(i-i')^2}{0.1}\right)$$

and the weight matrices in space are given by

$$w_{x,x'}^{V4gain/x} = 0.1 \exp\left(-\frac{(x_1-x'_1)^2 + (x_2-x'_2)^2}{0.005}\right).$$

For the colour channels H is defined as

$\forall d, i, x:$

$$\begin{aligned} H_{d,i,x} &= r_{d,i,x}^{V4gain} \left(\frac{1}{\#i} \sum_{i'} r_{d,i',x}^{V4gain} + w_{inh}^{RF} \max_{x' \in RF(x)} (z_{d,x'}^{V4gainRF}) + w_{inh}^{map} z_d^{V4gain} \right) \\ &+ w_{f\,inh} \frac{1}{\#i} \sum_{i'} r_{d,i',x}^{V4gain}, \end{aligned}$$

where $\#i$ refers to the number of cells in the respective population. z is an inhibitory unit which receives its input from all cells enclosed by a given IT receptive field ($z_{d,x'}^{V4gainRF}$) or from all cells in the map (z_d^{V4gain}) with

$$\tau^z \frac{\partial z_{d,x'}^{V4gainRF}}{\partial t} = \sum_{x'' \in RF(x')} \max_{i'} \left(r_{d,i',x''}^{V4gain} \right)$$

and

$$\tau^z \frac{\partial z_d^{V4gain}}{\partial t} = \sum_{x'} \max_{i'} \left(r_{d,i',x'}^{V4gain} \right).$$

Inhibitory neurons are simulated as described in Hamker (2005a) with a time constant of $\tau^z = 0.01s$. The inhibitory neurons of all other maps are modelled as with V4gain.

The following parameters were used:

$$\begin{aligned} \tau^{V4gain} &= 0.015s; w_{f\,inh} = 0.7; A = 1.2; w^{FEFvm-V4gain} = 3; \\ w^{IT-V4gain} &= 4; w_{inh}^{map} = \frac{3.2}{\#V4gain}; \\ w_{inh}^{RF} &= \frac{72}{\#V4gain}; w^{V4in-V4gain} = 0.7. \end{aligned}$$

Inferior temporal cortex (IT)

The change in firing rate of IT cells is computed as follows. The excitatory term G consists of the feedforward influence from V4gain (Eqn 2, line 1), the self-excitation among features and spatial location (Eqn 2, line 2) and the feature-based feedback from the target template in PF (Eqn 2, line 3).

$$\tau^{IT} \frac{\partial r_{d,i,x}^{IT}}{\partial t} = G - H; \quad r = (r)^+;$$

$\forall d, i, x:$

$$\begin{aligned} G_{d,i,x} &= w^{V4gain-IT} \max_{x' \in RF(x)} \left(r_{d,i,x'}^{V4gain} \right) \\ &+ w^{V4gain-IT} \max_{x' \in RF(x)} \left(r_{d,i,x'}^{V4gain} \right) \left(\sum_{i'} w_{i,i'}^{IT/i} r_{d,i',x}^{IT} \right) \\ &+ \left(A - \max_{i'} \left(r_{d,i',x}^{IT} \right) \right) + \max_{x' \in RF(x)} \left(r_{d,i,x'}^{V4gain} w^{PF-IT} r_{d,i}^{PF} \right) \quad (2) \end{aligned}$$

The weight matrices in feature space are constructed by

$$w_{i,i'}^{IT/i} = 0.35 \exp\left(-\frac{(i-i')^2}{0.05}\right).$$

For the colour channels H is defined as

$\forall d, i, x:$

$$H_{d,i,x} = r_{d,i,x}^{IT} \left(w_{inh} \sum_{i'} r_{d,i',x}^{IT} + w_{inh}^{map} z_d^{IT} \right) + w_{f\,inh} z_d^{IT}.$$

The following parameters were used:

$$\begin{aligned} \tau^{IT} &= 0.015s; A = 1.2; w_{inh} = \frac{3}{\#i}; w_{f\,inh} = 1.5; w^{V4gain-IT} = 0.6; \\ w^{PF-IT} &= 2; w_{inh}^{map} = \frac{3}{\#IT}. \end{aligned}$$

FEF visual (FEFv)

The FEFv map receives afferents from V4gain at the same location, irrespective of the non-spatial feature information, and thus encodes the conspicuity of locations. This representation is often referred to as a saliency map.

$$\tau^{FEFv} \frac{\partial r_x^{FEFv}}{\partial t} = G - H; \quad r = (r)^+;$$

$\forall x:$

$$G_x = \left(1 + \sum_{x'} w_{x,x'}^{FEFv/x} r_{x'}^{FEFv} \right) \left(w^{V4gain-FEFv} \sum_{d'} \max_{i'} \left(r_{d',i',x}^{V4gain} \right) \right)$$

$$\text{with } w_{x,x'}^{FEFv/x} = 0.25 \exp\left(-\frac{(x_1-x'_1)^2 + (x_2-x'_2)^2}{0.004}\right)$$

$\forall x:$

$$H_x = \left(r_x^{FEFv} + w_{f\,inh} \right) w_{inh}^{map} z^{FEFv}$$

The following parameters were used:

$$\tau^{FEFv} = 0.01s; w_{f\,inh} = 0.07; w^{V4gain-FEFv} = 0.06; w_{inh}^{map} = \frac{50}{\#FEFv}.$$

FEF visuomovement (FEFvm)

The FEFvm map receives input from FEFv and FEFm. For each location we simulate several neurons ($\#j = 5$) differing in the strength of their excitatory inputs from FEFv, resulting in a continuum of visual- and movement-related cells in FEFvm. The connections from FEFv to FEFvm are modelled by a difference of Gaussian functions (DOGs) reinforcing spatially nearby locations and inhibiting spatially distant ones. The average of all FEFvm cells j at a given location x in the map is fed back to V4gain.

$$\tau^{\text{FEFvm}} \frac{\partial r_{j,x}^{\text{FEFvm}}}{\partial t} = G - H; \quad \bar{r}_x^{\text{FEFvm}} = \frac{1}{\#j} \sum_j r_{j,x}^{\text{FEFvm}} \quad r = (r)^+;$$

$\forall j, x:$

$$G_{j,x} = \sum_{x'} w_{x,x',j}^{\text{FEFv-FEFvm}} r_{x'}^{\text{FEFv}} + w^{\text{FEFm-FEFvm}} r_x^{\text{FEFm}}$$

$\forall j, x:$

$$H_{j,x} = w_{\text{inh}}^{\text{map}} z^{\text{FEFvm}}$$

$\forall x, x', j:$

$$w_{x,x',j}^{\text{FEFv-FEFvm}} = g(x, x', a^+ s^{j-1}, \sigma^+) - g(x, x', a^-, \sigma^-)$$

$$g(x, x', a, \sigma) = \frac{a}{\sigma \#x_1^{\text{FEFvm}} 2\pi} \exp\left(-\frac{(x_1 - x'_1)^2 + (x_2 - x'_2)^2}{2(\sigma \#x_1^{\text{FEFvm}})^2}\right)$$

The function g denotes a two-dimensional Gaussian function. Its width is normalized to the width of the FEFvm map ($\#x_1^{\text{FEFvm}} = 50$).

The following parameters were used: $\tau^{\text{FEFvm}} = 0.01$; $w^{\text{FEFm-FEFvm}} = 0.9$; $w_{\text{inh}}^{\text{map}} = 0.01$.

Parameters for the positive part of the DOGs are the scale factor $a^+ = 6$ and the standard deviation $\sigma^+ = 0.0416$. Parameters for the negative part of the DOGs are $a^- = 0.75$ and $\sigma^- = 0.83$. Depending on the neuron j at one location, the DOGs have different positive peaks modulated by s^{j-1} with $s = 0.9$.

FEF movement (FEFm)

The FEFm map represents cells which encode saccade target information. The map has afferent and efferent connections to FEFvm.

$$\tau^{\text{FEFm}} \frac{\partial r_x^{\text{FEFm}}}{\partial t} = G - H; \quad r = (r)^+;$$

$\forall x:$

$$G_x = \left(1 + \sum_{x'} w_{x,x'}^{\text{FEFm/x}} r_{x'}^{\text{FEFm}} \right) \left(w^{\text{FEFvm-FEFm}} r_x^{\text{FEFvm}} - w_{\text{inh}}^{\text{FEFvm-FEFm}} \sum_{x'} r_{x'}^{\text{FEFvm}} \right)$$

$\forall x:$

$$H_x = r_x^{\text{FEFm}} \left(w_{\text{inh}}^{\text{map}} \left(1 + \sum_{x'} r_{x'}^{\text{FEFm}} \right) + w^{\text{Fix-FEFm}} r_{\text{Fix}} \right)$$

$$\text{with: } w_{x,x'}^{\text{FEFm/x}} = 0.9 \exp\left(-\frac{(x_1 - x'_1)^2 + (x_2 - x'_2)^2}{0.004}\right)$$

The strength of the responses in the FEFm map can be influenced by a so-called fixation cell, which is supposed to reflect the task at hand, i.e. covert vs. overt visual search. For all reported simulations

the impact of the fixation unit was adjusted to result in complete inhibition of all FEFm cells (Thompson *et al.*, 2005).

The following parameters were used:

$$\tau^{\text{FEFm}} = 0.02\text{s}; w^{\text{Fix-FEFm}} = 9; r^{\text{Fix}} = 12; w_{\text{inh}}^{\text{map}} = 0.005;$$

$$w_{\text{inh}}^{\text{FEFvm-FEFm}} = \frac{20}{\#\text{FEFm}}; w^{\text{FEFvm-FEFm}} = 0.5.$$

Prefrontal cortex (PF)

To simulate the instruction of the task ('searching for red'), we externally define the target template modulating the activity of $r_{d,i}^{\text{PF}}$. Note that for simplicity we did not use the option to encode the target into memory as used earlier in delayed match to sample tasks (Hamker, 2005b). As a result the target template leads to a bias in the IT population, i.e. a gain modulation of those cells that match the target template. This advantage for some cells can further be transferred by feature-specific feedback connections from IT to V4.

Stimuli and conditions

In Bichot *et al.* (1999) the subjects' primary task was to compare (same vs. different) the shape (unfilled circle vs. unfilled rectangle) of two of eight stimuli. The two target stimuli were identified by their identical colour (e.g. red), as given by instruction. The six remaining distractor stimuli had a different uniform colour (e.g. green). All stimuli were arranged on a circle around the point of fixation and were presented for 165 ms. After a fixed period of 105 ms with respect to the onset of the shape stimuli, letters were briefly (60 ms) shown inside each of the eight shapes and the subjects' secondary task was to report as many letters as possible irrespective of whether they were shown inside a target or a distractor as defined by the primary task. Thus, the idea of the secondary task (letter report) was to probe the amount of spatial attention elicited by the primary task. The crucial finding of this experiment was a superior performance in the secondary task for letters presented inside the two target shapes. This was even true when the targets were separated by one or more intervening distractors.

In an extension of the experiment by Bichot *et al.* (1999) in which only a fixed interval between cue onset and probe onset has been used, Dubois *et al.* (2009) introduced a variable stimulus onset asynchrony (SOA) similar to that (105 ms) used by Bichot *et al.* (1999). As in Bichot *et al.* (1999) the performance in the primary task, i.e. the form discrimination of the target stimuli, was high demonstrating the effectiveness of the colour cueing. For the secondary task, again, performance was poor for letters presented inside distractors while it was considerably higher for letters presented inside target stimuli. Furthermore, by means of a sophisticated statistical model Dubois *et al.* (2009) were able to demonstrate that letter identification at the target stimuli depended critically on the length of the SOA. For short SOAs (≤ 107 ms) a simultaneous increase in performance at both target positions was reported. For longer SOAs (> 107 ms), however, the performance at one of the targets was increasing while performance at the other target started to decrease, leading to a significant separation in performance between the two targets.

To simulate the principal finding of Dubois *et al.* (2009) with the present model, we simplified the stimuli as follows. As the critical manipulation of the experiment is the cueing of target locations by colour while shape is non-informative across targets and distractors, all simulations were done using rectangular location cues exclusively (P1 to P8; Fig. 2). The identification of letters requires more specialized filters than those currently implemented in the model. Therefore, to probe the

amount of attention directed toward a given location we used yellow squares, in the following referred to as *probes*, that were presented inside each cue. As the model was biased to ‘search’ for red, a red cue will be called *target* and a green cue *distractor*. We ensured that targets and distractors did not cause a response in the blue–yellow channel and probes did not cause a response in the red–green channel, so that target and probes do not directly interfere in V4. Thus, we probed the influence of attention on the representation of orthogonal stimuli in model V4 with respect to colour.

The timing of the stimuli was as follows. We used eight different SOAs (40, 53, 80, 107, 133, 160, 187 and 213 ms) describing the time between target onset and probe onset. The probes were presented for 60 ms followed by a blank until a total simulation duration of 350 ms was reached.

To explore further the conditions of selection beyond the cases considered by Dubois *et al.* (2009), a series of conditions was simulated by varying the number of targets and distractors. In the *no-target* condition all cues were green. In the *one-target* and *two-target* conditions, one and two targets, respectively, were red while the remaining distractors were green. Finally, we simulated a variant of the one-target condition leaving one distractor, but not the probe, out.

Results

We focus here on the models FEFvm and V4gain. Consistent with Thompson *et al.* (2005), model FEFm neurons were silent for all reported simulation results. As we do not model early visual processes as a dynamic system we show all model activities delayed by 50 ms with respect to stimulus presentation in order to be more consistent with typical neural latencies and thus to facilitate a comparison with electrophysiological data.

We first illustrate the general dynamics of the FEFvm cells during the one-target condition (Fig. 3) for an SOA of 133 ms. Initially, the

presentation of the cues causes similar activations at non-contiguous locations in the FEFvm map. However, due to the top-down feature bias for red, the population response corresponding to P7 becomes stronger over time while responses corresponding to distractor positions become inhibited. Furthermore, the inhibition is not uniform among all distractors. Whereas the responses corresponding to distractors shown at P2, P3, P4, P5 and P8 are largely reduced at 160 ms, responses corresponding to distractors shown at P1 and P6 maintain a high level. This is due to the strong feedforward competition in the FEFvm map, which largely magnifies even minor differences in the input. As the competition in the map depends strongly on the overall activity, the presentation of the probes further enforces the inhibitory mechanism, eventually resulting in an almost complete suppression of all distractor-related activity while the target-related activity reaches its maximum.

Figure 4 shows the activity traces of the one-target condition for all SOAs for FEFvm and V4gain cells. Again the target was presented at P7 and its corresponding population activity is depicted in red while the average distractor-related activity is depicted in blue. The displayed V4gain activity corresponds to the blue–yellow channel which responds only to the presentation of the probes. As can be observed for all SOAs, the target-related population response in both FEFvm and V4gain is considerably larger than the average distractor response. The effects of the competition in FEFvm increase as a function of the SOA, leading not only to an enhancement of the V4gain population activity at P7 but also to a suppression of the population responses at distractor positions. Thereby, this differential effect is largest for the four shortest SOAs (40–107 ms) and saturates for longer SOAs. Thus, by means of a continuous feedback to spatially overlapping V4gain populations the competition in the FEFvm map leads to a corresponding location bias of the probe response in V4gain. This bias is absent in the no-target condition where the cue array consists exclusively of distractors (Fig. 5). For all SOAs, the FEFvm and V4gain population response corresponding to P7 is now close to the average distractor response. The greater variability of the distractor responses in FEFvm as compared with V4gain is due to the stronger competitive dynamics of the former leading to relatively large amplifications of minor differences in the input signal. Figure 6 shows a direct comparison between the target-related FEFvm activity in the one-target (solid lines) and the no-target condition (dashed lines), resembling qualitatively the FEF recordings reported by Monosov & Thompson (2009). In this study monkeys had to respond to a leftward or rightward oriented Landolt C, the target. The target Landolt C and distractor Landolt C’s (upward or downward oriented) were presented inside coloured rings, where the colour served as a cue. The reaction time was much shorter when the target was presented in a red ring (valid cue condition) with other rings being all green as compared with a neutral cue condition when all rings were green. In the valid cue condition FEF neurons showed an early target effect after cue onset, which has been interpreted as the cause for the speeded response to the target.

The results of the two-target condition are shown in Fig. 7. In addition to the target presented at P7 a second target was presented at P3. As can be observed for all SOAs, the FEFvm activity related to both targets depicted in red and orange respectively is higher than the average distractor activity depicted in blue. For the two shortest SOAs the target-related activities increase simultaneously with a slight lead for P3. At an SOA of 80 ms the activity of the two targets is very similar. For longer SOAs, however, the activity related to stimuli presented at P7 becomes continuously stronger in the later part of the response while the response to stimuli at P3 becomes increasingly inhibited. This differential effect is also immanent in the V4gain

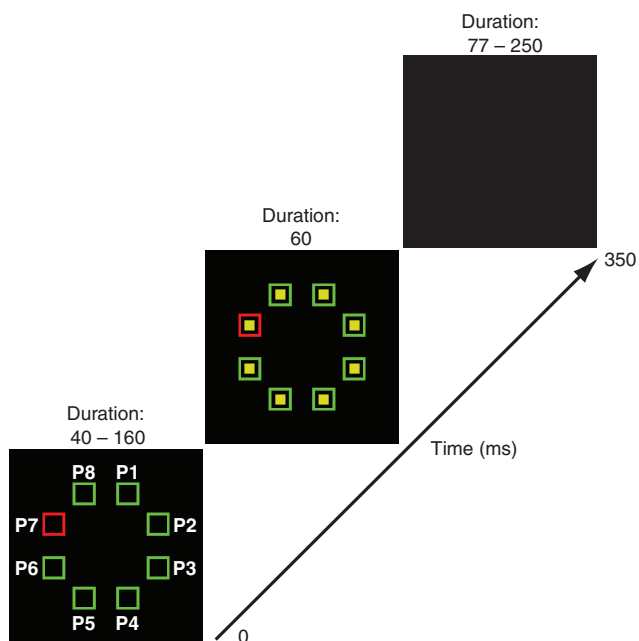


FIG. 2. Stimulus layout and timing. The visual input of the model consists of eight (P1–P8) rectangles, referred to as cues, arranged on a circle. After a variable time ranging from 40 to 213 ms a yellow square, referred to as probe, was shown inside each cue for 60 ms followed by a blank interval. A red cue defines a target whereas a green cue defines a distractor.

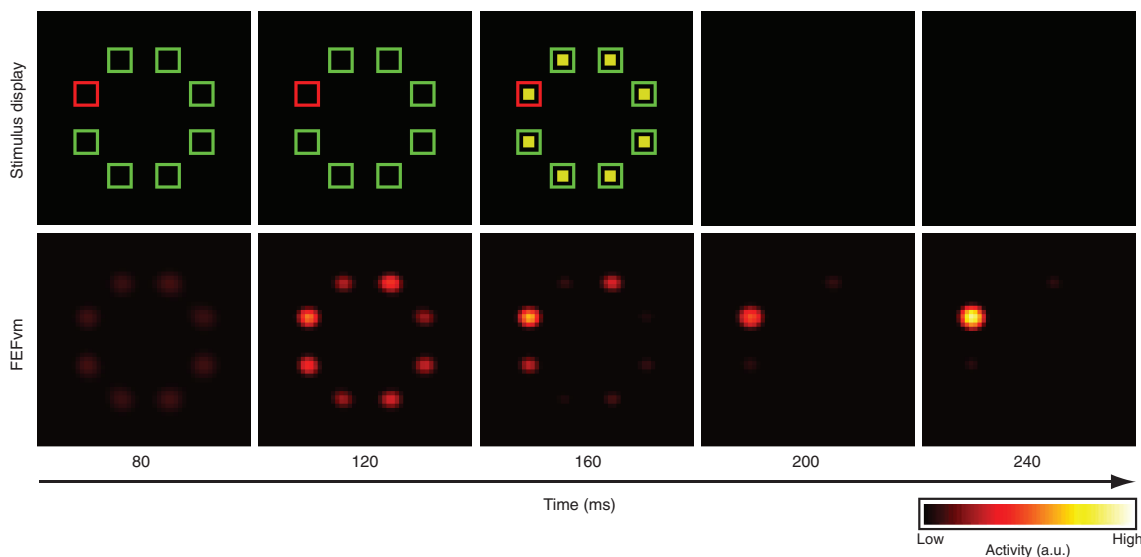


FIG. 3. Illustration of FEFvm dynamics in the one-target condition for an SOA of 133 ms. The actual presentation of stimuli at the selected points in time is shown in the upper row while the corresponding activity maps are shown in the lower row. P7 is cued as target (red rectangle) while all other positions are cued as distractors (green rectangles).

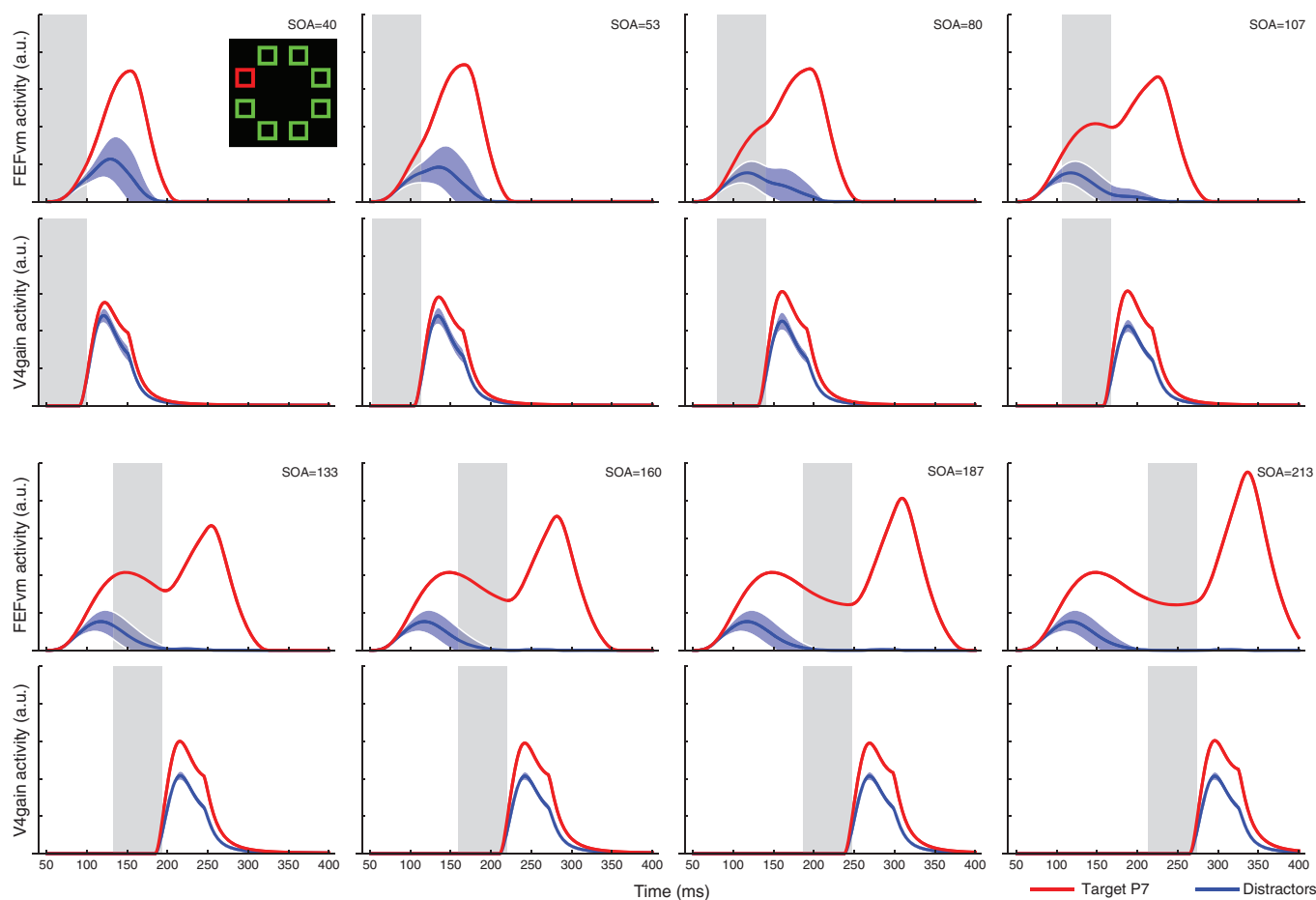


FIG. 4. FEFvm and V4gain activity obtained in the one-target condition. The panels of the FEFvm show the neural activity towards cues and probes whereas in V4gain to the probes only for all SOAs. The red line indicates the population response over time corresponding to P7 and the blue line indicates the average population response corresponding to all other locations. The blue area around the average response indicates ± 1 SD. The grey area in each panel indicates probe presentation.

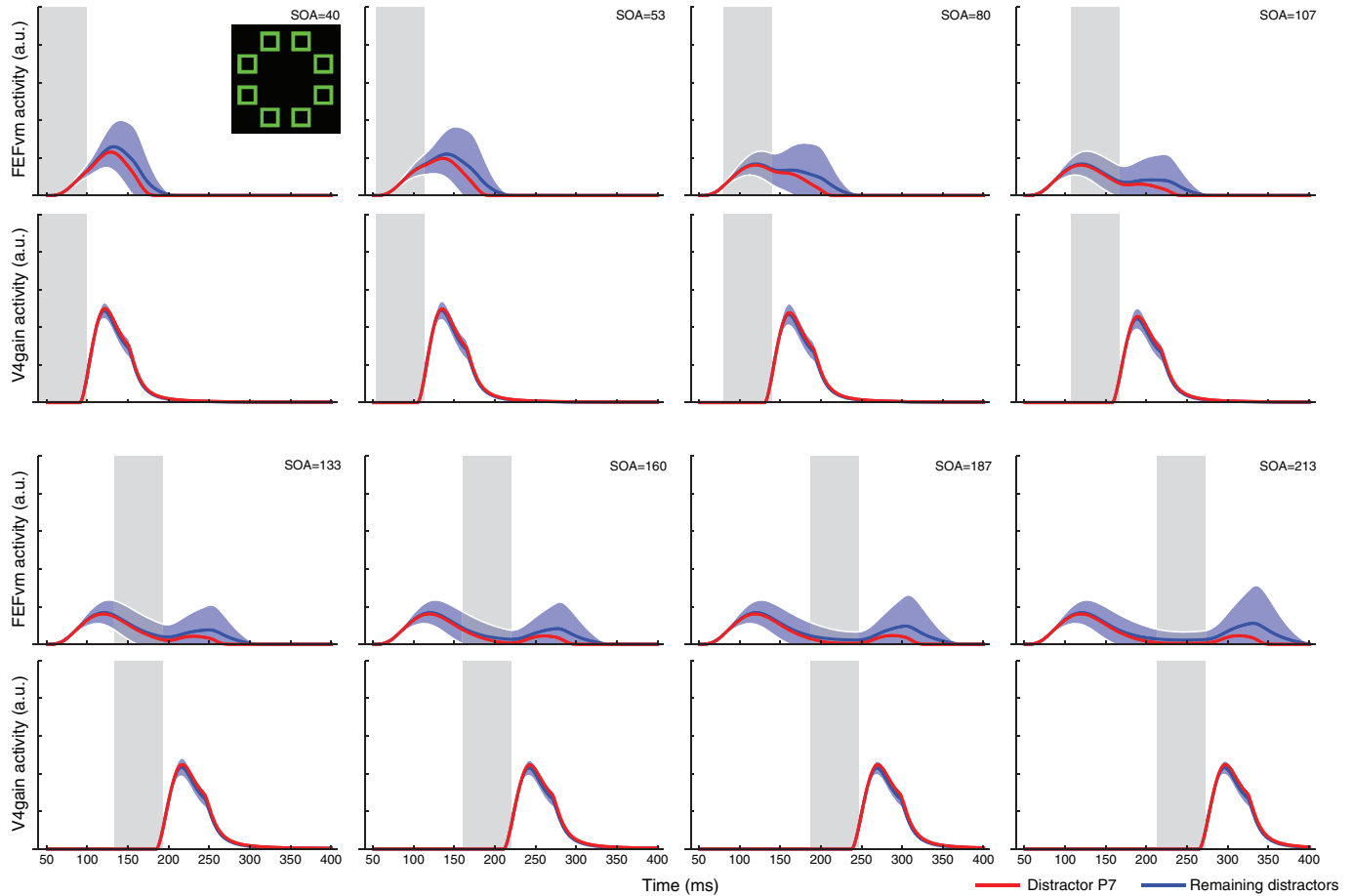


FIG. 5. FEFvm and V4gain activity obtained in the no-target condition. The panels of the FEFvm show the neural activity towards cues and probes whereas in V4gain to the probes only for all SOAs. The red line indicates the population response over time corresponding to P7 and the blue line indicates the average population response corresponding to all other locations. The blue area around the average distractor response indicates ± 1 SD. The grey area in each panel indicates the probe presentation period.

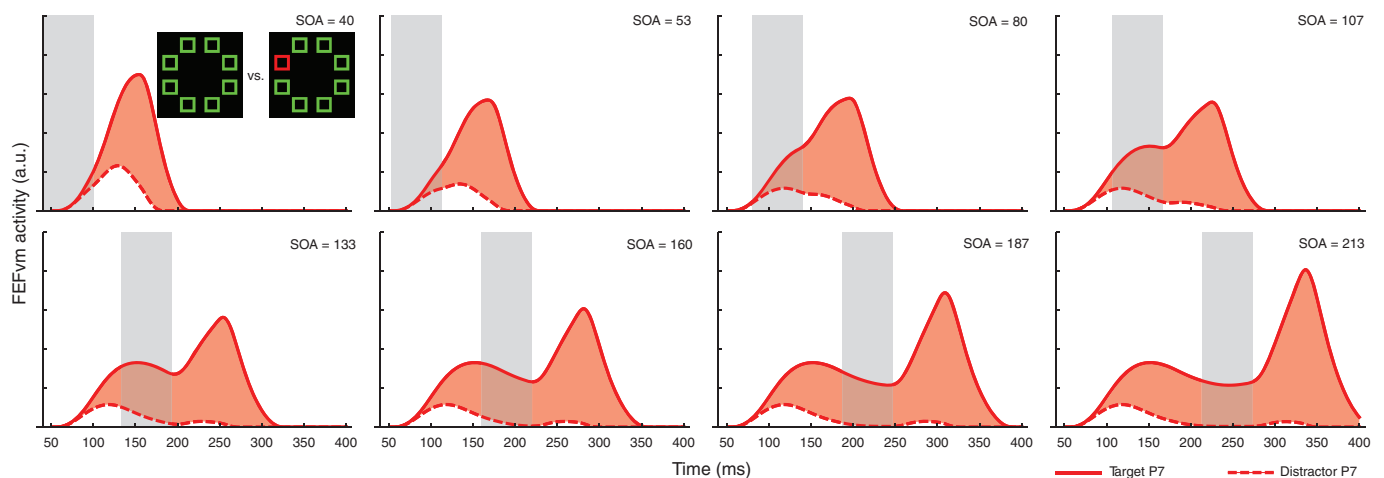


FIG. 6. Comparison between FEFvm activity obtained in the no-target and one-target condition. The panels show the activity of the FEFvm population at P7 for all eight SOAs. Solid lines indicate the population response over time in the no-target condition and dashed lines the population response in the one-target condition. The grey area in each panel indicates probe presentation.

responses. For the two shortest SOAs both responses are above the average response at distractor positions. For longer SOAs the V4gain response to probes presented at P7 remains high while the response

corresponding to probes presented at P3 becomes continuously smaller and is close to the average response at distractor positions for the largest SOA. Note the FEFvm response is the result of non-

linear competitive interactions and is triggered by the cue and probe stimuli. As we operate with real world scenes and compute saliency by subtracting subsampled versions of the original images (the surround), each stimulus does not necessarily activate the neurons at an identical level. This explains why an initial bias at one target can be overwritten by a bias to the probe at the other target. These biases introduce variations, but repeated simulations showed that such biases do not affect the basic results and predictions.

A comparison of the results for V4gain as obtained in all three conditions (no-target, one-target and two-target) is shown in Fig. 8. The displayed activities are integrated over time and normalized within each SOA. In the no-target condition (Fig. 8A) the response measured at P7 (red curve) is in the range of the normalized response averaged across all remaining distractor positions (depicted in blue). In the one-target condition (Fig. 8B) the activity for probes presented at P7 is substantially higher than those of the distractor positions and increases as a function of SOA. In the two-target condition (Fig. 8C) the activity corresponding to probes presented at both target locations, P7 depicted in red and P3 depicted in orange, increases initially similarly. At an SOA of 107 ms, however, the activity related to probes at P3 starts to decrease while the activity related to probes at P7 further increases. To summarize, in V4gain, the cuing of two targets leads to similarly enhanced responses to probes presented inside the targets for short SOAs. This result qualitatively reproduces the simultaneous split of attention for short SOAs as reported by Dubois

et al. (2009). It also shows that this split is transient rather than sustained due to the competitive interactions in the network.

Finally, the model predicts that the response to probes in early visual areas such as V4gain are higher at distractor locations than at uncued positions. We simulated the one-target condition subsequently leaving one of the distractors out while all probes were presented (Fig. 9). Solid lines indicate the model V4gain responses to probes presented inside distractors and dashed lines indicate V4gain responses to probes presented at uncued positions. Responses to probes presented inside distractors are higher than responses to probes presented at uncued positions for short SOAs (40–107 ms) and approximately equal for longer SOAs. This is due to the initial response the distractors cause in the FEFvm, which is continuously fed back to V4gain. For longer SOAs, however, the FEFvm responses to distractors become gradually suppressed due to the increased activation of the population encoding the target, leading to a diminished feedback signal at all other locations.

Discussion

The focus of the present study has been to offer a possible explanation for the psychophysical observation of a transient split of spatial attention in humans (Dubois *et al.*, 2009) while relying on recent observations in monkey FEF (Monosov & Thompson, 2009). In above two studies spatial position was cued by the colour of unfilled shapes.

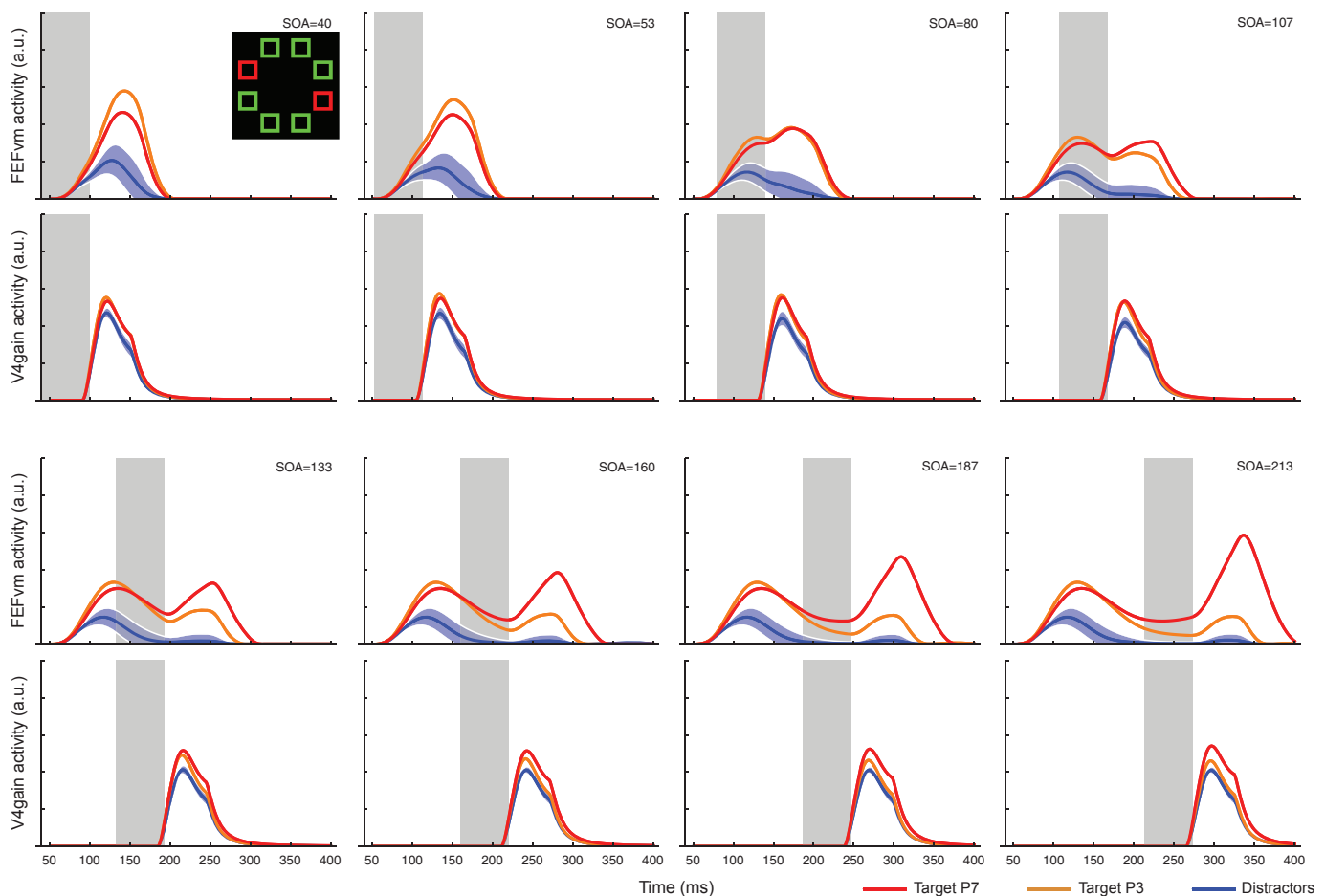


FIG. 7. FEFvm and V4gain activity obtained in the two-target condition. The panels of the FEFvm show the neural activity towards cues and probes whereas in V4gain to the probes only for all SOAs. The red line indicates the population response over time corresponding to P7, the orange line the population response corresponding to P3, and the blue line the average population response corresponding to all other locations. The blue area around the average distractor response indicates ± 1 SD. The grey area in each panel indicates probe presentation.

In our model this colour cuing, as implemented by a top-down feature-specific bias (assumed to reflect the cognitive task set), leads to an early advantage and separation in terms of the neural activity of targets and distractors, a result similar to findings reported by Bichot *et al.* (1996) and Bichot & Schall (2002) in the FEF. This initial separation, in the model, is further magnified by re-entrant processing – continuously feeding back the FEF activity and resulting in a space-specific bias, enhancing the corresponding activity in V4 which is again projected to the FEF. Although for short SOAs a simultaneous increase of cell populations encoding both targets in the two-target condition can be observed, the competitive interactions at various levels of the system (Kastner & Pinsk, 2004) lead to a gradually increasing separation between the targets for larger SOAs (≥ 107 ms).

Research on attention has been much influenced by the idea of a spotlight and a multitude of attentional phenomena have often been

described in qualitative terms. However, without a close consideration of the neural correlates, attention cannot really be constrained and arbitrary shaped foci can be taken into account such as elliptic foci to argue against a split of attention (e.g. Jans *et al.*, 2010). Computational approaches, particularly when linked to neuroanatomical and physiological observations, have the advantage of making more precise assumptions about the underlying mechanisms. Although a number of models have been proposed (for an overview see Itti *et al.*, 2005; Hamker, 2005b) most of them offer no intuitive explanation for the observation of a transient split of spatial attention as reported by Dubois *et al.* (2009). For example, present models relying on spatial selection as determined by a single winner in some kind of high-level salience map (Itti & Koch, 2000; Koch & Ullman, 1985; Treisman & Gelade, 1980; Wolfe, 1994; for a review see Itti & Koch, 2001), do not account for the dynamic part of the selection process. That is, even if

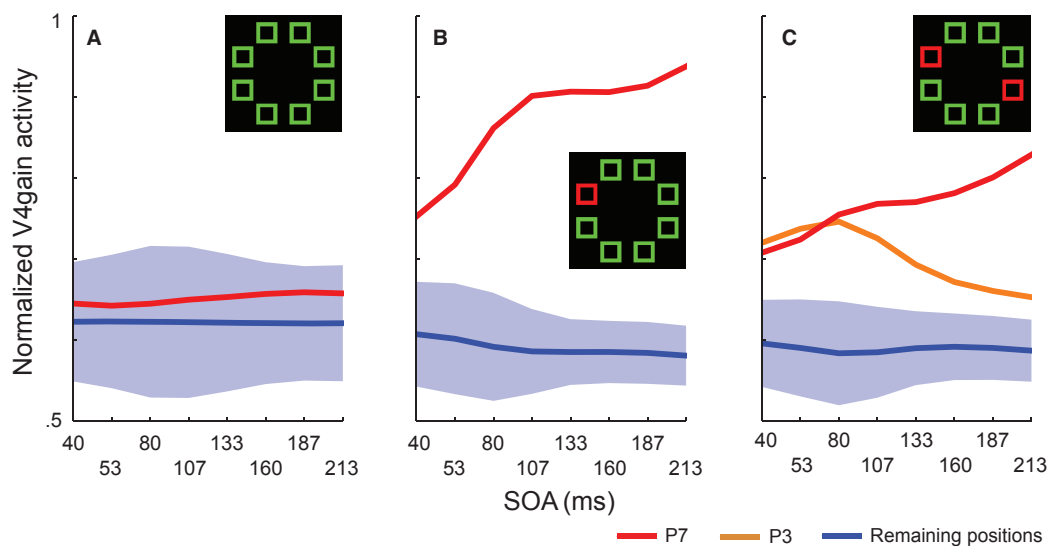


FIG. 8. V4gain activity as a function of SOA. (A) Results of the no-target condition. The red line indicates the population response corresponding to the probe presented inside the distractor at P7. The blue line indicates the average population response to probes presented inside all other distractors. The blue area around the average distractor response indicates ± 1 SD. (B) Results of the one-target condition. The red line indicates the population response corresponding to the probe presented inside the target at P7. (C) Results of the two-target condition. The orange line indicates the population response corresponding to the probe presented inside the target at P3. Note the displayed activities are integrated over time and normalized within each SOA.

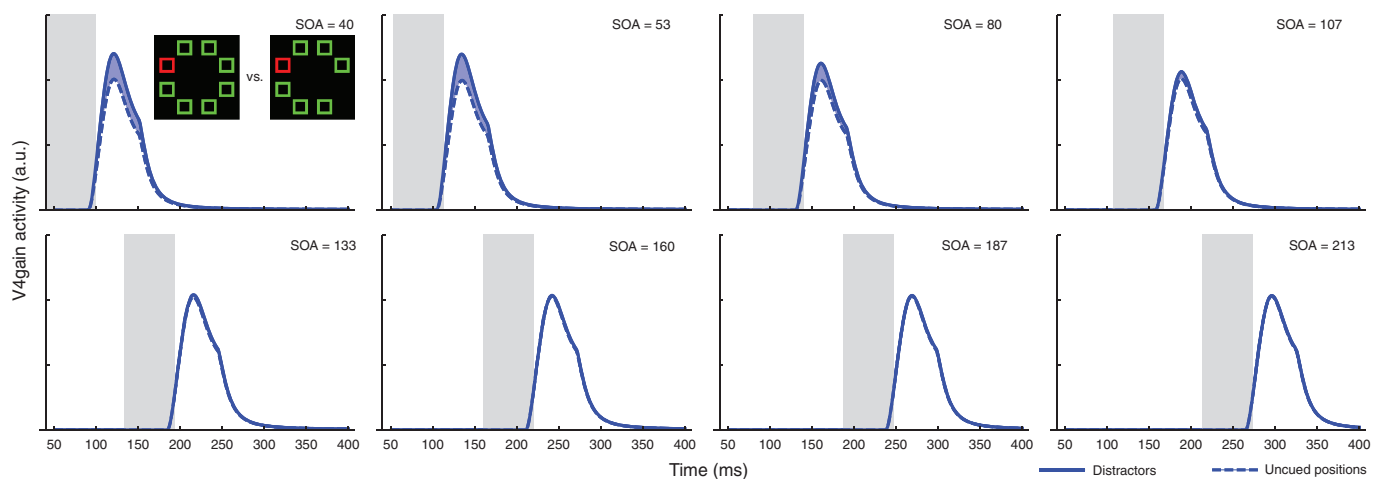


FIG. 9. Comparison between responses to probes presented inside distractors and to probes presented at uncued locations. The model predicts early transient attention effects at distractor locations. The panels show the activity of the population response to probes in V4gain for all SOAs. The solid line indicates the average population response to probes presented inside distractors and the dashed line indicates the average population response to probes presented at uncued positions. The grey area in each panel indicates the probe presentation period. The displayed activities are integrated over time and normalized within each SOA.

they were allowing for multiple winners (e.g. Tsotsos *et al.*, 1995), i.e. multiple locations at which spatial attention is engaged thereafter, they neglect the possibility that salience itself might be dynamically subject to change in the course of a spatial selection process. An interesting conceptual extension of the saliency map model has been proposed by Standage *et al.* (2005) using neural fields which naturally converge to a stable state, resulting in multiple local activity hills, where the number and position of the hills depends on the lateral inhibitory connectivity. However, it is not clear how this model maps on specific brain areas.

Our proposed model offers an account for a more dynamic view on attention. After the initial salience is computed from the input image it is gradually updated by the competitive model dynamics. Such dynamics can be very flexible, they depend on the task and the particular stimulation. Despite the nice, intuitive analogy between attention and a spotlight, a more detailed description of attention refines this simplified view to a more dynamic and gradual process, where focused processing of a particular single location is rather the final state of a longer process to extract specific information at that location. Although we assume that the FEF plays a major role in orienting spatial attention, we do of course not mean that all attentional effects are mediated by the FEF. However, feedback from the FEF as modelled here provides a simple explanation for the psychophysical observations provided by Dubois *et al.* (2009) without relying on the assumption of complex, arbitrary shaped spotlights for a transient split of attention.

If we adopt the idea of attention as a product of re-entrant processing, the issue of target selection in the FEF and the source of re-entrant processing is of major relevance. Recent experiments reported a dissociation between selection and movement preparation (Sato & Schall, 2003; Juan *et al.*, 2004; Ray *et al.*, 2009). Moreover, it has been shown that during covert visual search visually responsive FEF neurons showed differential activity between target and distractor while movement neurons were inhibited (Thompson *et al.*, 2005). Although previous versions of our model (e.g. Hamker, 2006) show attentional selection with inactive movement cells as well, this selection is mediated by feature-specific signals and is already present in the input of the FEF. Thus, target selection in terms of an enhanced activity of visual selective FEF neurons does not unambiguously provide evidence for a causal role in the deployment of spatial attention *per se*, but also requires demonstration that this enhanced activity does improve target discrimination or at least affect the neural response in areas involved in feature discrimination such as V4. Thus far, the strongest support for a direct role of visual selective FEF neurons in spatial attention comes from recent neuroanatomical findings (Pouget *et al.*, 2009) showing that the projection from FEF to SC originates in layer 5 while the projection from FEF to V4 and area TEO originates in layer 2/3 and layer 5, but without the observation of double labelled cells in layer 5. This suggests a separation between the pathways to SC and V4, but it does not mean that FEF cells with pure movement characteristics do not project to V4 and TEO. To our knowledge, there exists no strong conclusion regarding this issue. Furthermore, the term visuomovement describes a set of cells of a continuum ranging from only weak visual responses and strong saccade-related responses and to the opposite. Thus, to answer the question about the nature of the feedback (visual or motor), the population response characteristics of FEF cells projecting back to visual areas must be known. Recent simulations have shown that strong pre-saccadic motor-related feedback to earlier visual areas explains the peri-saccadic mislocalization of briefly flashed stimuli (Hamker *et al.*, 2008), a phenomenon that has not previously been related to

attention. We believe that studies addressing these questions will be of great value to further constrain future models of attention.

To summarize, in this study we demonstrated that feedback from visuomovement cells as implemented in our model is able to account for a transient split of spatial attention in terms of an enhanced activity of both FEF_{vm} and V4_{gain} neurons corresponding to target stimuli. As with the behavioural results (Dubois *et al.*, 2009) this split of attention in the model is dynamic in the sense that it builds up for short SOAs and then gradually decreases for longer SOAs due to the increased competition in the system. Our simulations show that by continuously feeding back the activity of the FEF_{vm} we were able to demonstrate the build up of two preferentially processed locations within a single salience map, enhancing the activity of corresponding V4_{gain} populations. While spatial feedback from movement cells can also cause a split of attention (Hamker, 2004a), the assumption that spatial attention is deployed by visuomovement cells leads to the prediction of a transient enhancement of stimuli presented at distractor locations as compared with uncued locations. That is, in our revised model spatial attention is initially also directed to distractor locations due to the phasic onset response of the visuomovement cells. This prediction underlines the conceptual framework according to which attention emerges by competitive interactions within different brain areas rather than by an explicit selection within a particular salience map and emphasizes the gradual aspect of attention-related modulations on the neurophysiological level as compared with an all-or-none selection. Thus, in contrast with more static views of attentional selection focusing rather on the final outcome, i.e. a final location in space that has been singled out, our framework stresses the dynamic aspect of continuous attentional deployment mediated by spatial- and feature-based feedback signals.

Is a split of attention inherently transient? In our simulations, the split of attention is limited to short SAOs while for longer SOAs the model dynamics effectively settle down on a single target. This is an inherent prediction of the model which only partially depends on the chosen parameters. However, we do not want to exclude the possibility of longer sustained periods of divided spatial attention at multiple locations (Muller *et al.*, 2003) and our present model is of course not intended to account for all results provided by the wide range of experimental paradigms studying the split of attention, particularly not for experiments that involve the monitoring of multiple locations for an extended period. Modelling such experiments would require us to include brain structures more involved in executive control and is beyond the scope of the present framework. However, we believe that observations of tonic activity at distinct locations in brain structures that are known to modulate the representation of stimuli in earlier visual areas will be necessary evidence for the existence of a sustained split of spatial attention.

Abbreviations

FEF, frontal eye field; IT, inferior temporal cortex; PF, prefrontal; SC, superior colliculus; SOA, stimulus onset asynchrony.

References

- Awh, E. & Pashler, H. (2000) Evidence for split attentional foci. *J. Exp. Psychol. Hum. Percept. Perform.*, **26**, 834–846.
- Bichot, N.P. & Schall, J.D. (2002) Priming in macaque frontal cortex during popout visual search: feature-based facilitation and location-based inhibition of return. *J. Neurosci.*, **22**, 4675–4685.

- Bichot, N.P., Schall, J.D. & Thompson, K.G. (1996) Visual feature selectivity in frontal eye fields induced by experience in mature macaques. *Nature*, **381**, 697–699.
- Bichot, N.P., Cave, K.R. & Pashler, H. (1999) Visual selection mediated by location: feature-based selection of non-contiguous locations. *Percept. Psychophys.*, **61**, 403–423.
- Bichot, N.P., Rossi, A.F. & Desimone, R. (2005) Parallel and serial neural mechanisms for visual search in macaque area V4. *Science*, **308**, 529–534.
- Brown, J.W., Bullock, D. & Grossberg, S. (2004) How laminar frontal cortex and basal ganglia circuits interact to control planned and reactive saccades. *Neural Netw.*, **17**, 471–510.
- Buffalo, E.A., Fries, P., Landman, R., Liang, H. & Desimone, R. (2010) A backward progression of attentional effects in the ventral stream. *Proc. Natl. Acad. Sci. USA*, **107**, 361–365.
- Burrows, B.E. & Moore, T. (2009) Influence and limitations of popout in the selection of salient visual stimuli by area V4 neurons. *J. Neurosci.*, **29**, 15169–15177.
- Cavanaugh, J., Alvarez, B.D. & Wurtz, R.H. (2006) Enhanced performance with brain stimulation: attentional shift or visual cue? *J. Neurosci.*, **26**, 11347–11358.
- Chelazzi, L., Duncan, J., Miller, E.K. & Desimone, R. (1998) Responses of neurons in inferior temporal cortex during memory-guided visual search. *J. Neurophysiol.*, **80**, 2918–2940.
- Dubois, J., Hamker, F.H. & VanRullen, R. (2009) Attentional selection of noncontiguous locations: the spotlight is only transiently ‘split’. *J. Vis.*, **9**, 3.
- Gobell, J.L., Tseng, C.H. & Sperling, G. (2004) The spatial distribution of visual attention. *Vision Res.*, **44**, 1273–1296.
- Grosbras, M.H. & Paus, T. (2002) Transcranial magnetic stimulation of the human frontal eye field: effects on visual perception and attention. *J. Cogn. Neurosci.*, **14**, 1109–1120.
- Hamker, F.H. (2003) The reentry hypothesis: linking eye movements to visual perception. *J. Vis.*, **3**, 808–816.
- Hamker, F.H. (2004a) A dynamic model of how feature cues guide spatial attention. *Vision Res.*, **44**, 501–521.
- Hamker, F.H. (2004b) Predictions of a model of spatial attention using sum- and max-pooling functions. *Neurocomputing*, **56C**, 329–343.
- Hamker, F.H. (2005a) The reentry hypothesis: the putative interaction of the frontal eye field, ventrolateral prefrontal cortex, and areas V4, IT for attention and eye movement. *Cereb. Cortex*, **15**, 431–447.
- Hamker, F.H. (2005b) The emergence of attention by population-based inference and its role in distributed processing and cognitive control of vision. *Comput. Vis. Image Underst.*, **100**, 64–106.
- Hamker, F.H. (2006) Modeling feature-based attention as an active top-down inference process. *BioSystems*, **86**, 91–99.
- Hamker, F.H., Zirnsak, M., Calow, D. & Lappe, M. (2008) The peri-saccadic perception of objects and space. *PLoS Comput. Biol.*, **4**, e31.
- Heinzle, J., Hepp, K. & Martin, K.A. (2007) A microcircuit model of the frontal eye fields. *J. Neurosci.*, **27**, 9341–9353.
- Itti, L. & Koch, C. (2000) A saliency-based search mechanism for overt and covert shifts of visual attention. *Vision Res.*, **40**, 1489–1506.
- Itti, L. & Koch, C. (2001) Computational modelling of visual attention. *Nat. Rev. Neurosci.*, **2**, 194–203.
- Itti, L., Rees, G. & Tsotsos, J.K. (eds) (2005) *Neurobiology of Attention*. Elsevier/Academic Press, New York.
- Jans, B., Peters, J.C. & De Weerd, P. (2010) Visual spatial attention to multiple locations at once: the jury is still out. *Psychol. Rev.*, **117**, 637–684.
- Juan, C.H., Shorter-Jacobi, S.M. & Schall, J.D. (2004) Dissociation of spatial attention and saccade preparation. *Proc. Natl. Acad. Sci. USA*, **101**, 15541–15544.
- Kastner, S. & Pinsk, M.A. (2004) Visual attention as a multilevel selection process. *Cogn. Affect. Behav. Neurosci.*, **4**, 483–500.
- Koch, C. & Ullman, S. (1985) Shifts in selective visual attention: towards the underlying neural circuitry. *Hum. Psychol.*, **4**, 219–227.
- Kramer, A.F. & Hahn, S. (1995) Splitting the beam: distribution of attention over noncontiguous regions of the visual field. *Psychol. Sci.*, **6**, 381–386.
- McAdams, C.J. & Maunsell, J.H. (1999) Effects of attention on orientation-tuning functions of single neurons in macaque cortical area V4. *J. Neurosci.*, **19**, 431–441.
- Monosov, I.E. & Thompson, K.G. (2009) Frontal eye field activity enhances object identification during covert visual search. *J. Neurophysiol.*, **120**, 3656–3672.
- Moore, T. & Armstrong, K.M. (2003) Selective gating of visual signals by microstimulation of frontal cortex. *Nature*, **421**, 370–373.
- Moore, T. & Fallah, M. (2001) Control of eye movements and spatial attention. *Proc. Natl. Acad. Sci. USA*, **98**, 1273–1276.
- Motter, B.C. (1994) Neural correlates of attentive selection for color or luminance in extrastriate area V4. *J. Neurosci.*, **14**, 2178–2189.
- Muggleton, N.G., Juan, C.H., Cowey, A. & Walsh, V. (2003) Human frontal eye fields and visual search. *J. Neurophysiol.*, **89**, 3340–3343.
- Muller, M.M., Malinowski, P., Gruber, T. & Hillyard, S.A. (2003) Sustained division of the attentional spotlight. *Nature*, **424**, 309–312.
- Muller, J.R., Philiastides, M.G. & Newsome, W.T. (2005) Microstimulation of the superior colliculus focuses attention without moving the eyes. *Proc. Natl. Acad. Sci. USA*, **102**, 524–529.
- Pouget, P., Stepniewska, I., Crowder, E.A., Leslie, M.W., Emeric, E.E., Nelson, M.J. & Schall, J.D. (2009) Visual and motor connectivity and the distribution of calcium-binding proteins in macaque frontal eye field: implications for saccade target selection. *Front. Neuroanat.*, **3**, 2.
- Ray, S., Pouget, P. & Schall, J.D. (2009) Functional distinction between visuomotor and movement neurons in macaque frontal eye field during saccade countermanding. *J. Neurophysiol.*, **102**, 3091–3100.
- Reynolds, J.H., Pasternak, T. & Desimone, R. (2000) Attention increases sensitivity of V4 neurons. *Neuron*, **26**, 703–714.
- Rizzolatti, G., Riggio, L., Dascola, I. & Umiltà, C. (1987) Reorienting attention across the horizontal and vertical meridians: evidence in favor of a premotor theory of attention. *Neuropsychologia*, **25**, 31–40.
- Sato, T.R. & Schall, J.D. (2003) Effects of stimulus-response compatibility on neural selection in frontal eye field. *Neuron*, **38**, 637–648.
- Segraves, M.A. & Goldberg, M.E. (1987) Functional properties of corticotectal neurons in the monkey’s frontal eye field. *J. Neurophysiol.*, **58**, 1387–1419.
- Silvanto, J., Lavie, N. & Walsh, V. (2006) Stimulation of the human frontal eye fields modulates sensitivity of extrastriate visual cortex. *J. Neurophysiol.*, **96**, 941–945.
- Smith, D.T., Jackson, S.R. & Rorden, C. (2005) Transcranial magnetic stimulation of the left human frontal eye fields eliminates the cost of invalid endogenous cues. *Neuropsychologia*, **43**, 1288–1296.
- Standage, D.I., Trappenberg, T.P. & Klein, R.M. (2005) Modelling divided visual attention with a winner-take-all network. *Neural Netw.*, **18**, 620–627.
- Taylor, P.C., Nobre, A.C. & Rushworth, M.F. (2007) FEF TMS affects visual cortical activity. *Cereb. Cortex*, **17**, 391–399.
- Thompson, K.G., Biscoe, K.L. & Sato, T.R. (2005) Neural basis of covert spatial attention in the frontal eye field. *J. Neurosci.*, **25**, 9479–9487.
- Treisman, A. & Gelade, G. (1980) A feature integration theory of attention. *Cogn. Psychol.*, **12**, 97–136.
- Tsotsos, J.K., Culhane, S.M., Wai, W., Lai, Y., Davis, N. & Nuflo, F. (1995) Modeling visual attention via selective tuning. *Artif. Intell.*, **78**, 507–545.
- Wolfe, J.M. (1994) Guided search 2.0: a revised model of visual search. *Psychon. Bull. Rev.*, **1**, 202–238.